MATHEMATICAL ANALYSIS OF CELL–TARGET ENCOUNTER RATES IN TWO DIMENSIONS

The Effect of Chemotaxis

ELIZABETH S. FISHER AND DOUGLAS A. LAUFFENBURGER
Department of Chemical Engineering, University of Pennsylvania, Philadelphia, Pennsylvania 19104

ABSTRACT The process by which cells encounter their targets is the first step of a number of cell functions involved in the immune response, such as cell-mediated cytotoxicity and phagocytic ingestion of foreign material. In many instances, this encounter may be rate-limiting, and therefore it is important to understand what factors influence the encounter rate.

One key aspect of cell–target encounter is the motility behavior of the cell in the vicinity of a target. This movement may be entirely random, or there may be a directed, or chemotactic, component to it. In this paper we focus on the effects of cell motility properties, and particularly the chemotactic directional bias, on the rate of cell–target encounter. Specifically, we derive an expression for the mean encounter time of cells that meet targets in two dimensions as a function of the cells' directional orientation bias. We show that a modest degree of bias can reduce the mean encounter time by orders of magnitude, while nearly perfect directional bias offers little additional benefit. We illustrate the application of these results to a particular example system: alveolar macrophages removing inhaled particles and bacteria from the lung surface.

INTRODUCTION

Many immunological processes require that cells come into contact with other cells or foreign particles. For example, cytotoxic T-lymphocytes and natural killer cells kill virus-infected or tumor cells. The mechanism of the lysis, or killing, is not known, but the process requires direct cell–target contact (6). Another example is the process of phagocytosis, the ingestion of particles and bacteria by cells such as neutrophils and macrophages (6). These cells must encounter their targets before they can ingest them. After consuming foreign material, macrophages can also activate T-lymphocytes through antigen presentation. This is a binding step, again requiring cell–cell contact, in which macrophages "present" the foreign material to the unactivated cell (26). Effective cell function thus not only depends on the cells' ability to perform the binding or killing steps but also on its efficiency in encountering a target.

The motility properties of some of the cells involved in these activities have been studied experimentally, and the cells have been observed to move with a directional bias in response to some chemical attractants (7, 9, 27, 32, 34, 36). These attractants include chemicals that could be produced by target cells and components of the complement cascade that are generated by the immune system at the surface of a foreign particle. Through binding of cell–surface receptors to such chemoattractants in the environment, cells can detect a gradient of chemoattractant and can orient themselves to move toward higher concentrations. This phenomenon is called chemotaxis. Despite its possible involvement in the processes mentioned above, the consequences of chemotaxis for the rates of encounter in vivo are not well understood.

One particular example that illustrates the importance of the encounter process is the system of phagocytic cells on the surface of the lung. These are pulmonary alveolar macrophages, and they maintain a resident population responsible for removing inhaled particles and bacteria from the lung surface (12, 28). The effectiveness of the alveolar macrophage in this clearance is known to depend on such factors as the initial numbers of bacteria and macrophages (30) and bacterial growth rates (11). It should also be affected by cell motility and chemotactic properties. Two observations that support this latter assertion concern the effects of age and of ozone exposure on the lung. It is known that exposure to high levels of ozone, which reduces alveolar macrophage migration rates (27), causes lung tissue damage and reduces the rate of bacterial clearance from the lung surface (11). The decreasing susceptibility of infants to bacterial lung infection may be linked to the observed increase in the chemotactic ability of their alveolar macrophages with time in their first few weeks of life (35). Insight into the effects that these factors have on macrophage–target encounter rate will allow their influence on the perfor-

mance of alveolar macrophages in the lungs to be assessed.

This paper investigates the effect of chemotactic directional bias in cell motion on the rate of encounter between cells and targets. A two-dimensional system is considered, both for conceptual simplicity and to allow for straightforward comparison to the example system of alveolar macrophage motion on the lung surface. An expression is derived for the mean time required for encounter to occur between a single cell and a target, and encounter times are calculated for alveolar macrophages reaching targets on the lung surface.

MATHEMATICAL MODEL

We wish to derive an equation governing the mean time required for a cell moving with directional bias in two dimensions to reach a target. This time is the average over all possible paths a cell can take from a particular starting position to the target. The encounter time calculated for a moving cell meeting a target is equivalent to the mean capture time that can be calculated for a moving particle being trapped by an absorber (3), or the mean first passage time calculated for a moving particle arriving at some position in space for the first time (10). In the situation described here, a fixed target is eliminated by a moving cell when the first encounter between cell and target occurs.

The cell is initially placed within a unit space of radius R that has a target at its center. Encounter occurs when the edge of the cell meets the edge of the target, or when their centers of mass are a distance A apart. This distance A is the contact radius and is equal to the sum of the radii of cell and target. For relatively small targets such as particles or bacteria, this quantity will be essentially equal to the cell radius, or the effective radius of the moving cell, as its membrane ruffles and it extends a pseudopod in the direction of motion (1, 31). The unit space is illustrated in Fig. 1.

When single cell–single target encounter is considered, the size of the unit space (the area surrounding one target) is equivalent to the total area available to the cell. If more than one target is present in the entire region of observation, the surface is essentially covered by adjacent unit spaces, and the size of the area surrounding each individual target will depend on the target surface density. For high target density, the average size of a unit space will be small, and under these conditions the time required for the cell to reach any target will be shorter than if the target density were low.

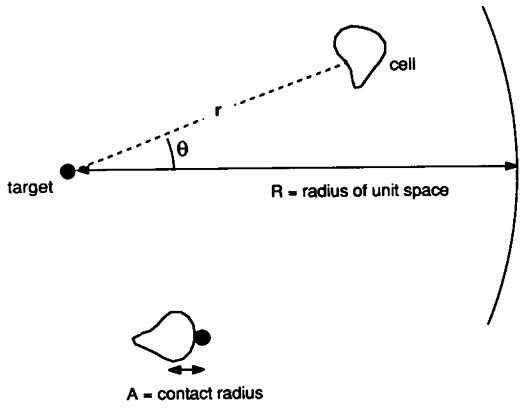

FIGURE 1. Diagram of the unit space.

One way to describe the size of a unit space is to assume that the targets are uniformly distributed on a surface, in which case the outer radius of a unit space is equal to half the average distance between targets. This makes the size of the unit space a function of the target density and will therefore make the encounter time an implicit function of target surface density. If there are T targets per unit surface area, then the number of targets in a unit space, 1, is equal to the product of the target surface density, T, and the area of the unit space:

$$1 = T(\pi R^2) \text{ or } R = 1/(\pi T)^{1/2}. \quad (1)$$

Under this assumption of uniform target distribution, our model provides an approximation to the actual encounter time that would be observed in a multiple target system. Other target distributions are possible, but would presumably lead to more complicated relationships between encounter time and target density. Berg and Purcell (3) calculate a current of ligand molecules encountering receptor molecules on the cell surface, and this current is only slightly smaller for randomly distributed receptors than it is for a uniform distribution of receptors. By analogy, it is likely that the average encounter time calculated for cells meeting randomly dispersed targets would not be much different than the time we calculate for uniformly distributed targets.

In the body, many immune cells search for their targets, but in the initial stages of infection, the cell density will usually be smaller than the target density. The effect of competition among cells should be negligible in this case, so our model for single cell encounter is expected to be valid. As targets are encountered and eliminated, or as more immune cells are recruited to the site of infection, the targets will be outnumbered. In this case it may be necessary to determine the size of the unit space from the cell surface density to account for cell–cell interactions.

The actual path traced out by a cell as it moves in the unit space is modeled as a series of steps. For simplicity, we assume that the cell takes steps in any of four perpendicular directions: toward or away from the target and in two directions lateral to the target. The size of a step is equal to the product of the cell speed and a characteristic "step time," τ, which will be assumed to be equivalent to the persistence time of the cell. This is the time between significant changes in direction of cell motion (8). Observations of polymorphonuclear leukocytes indicate that this

time between turns does not depend on either the presence of a gradient of chemoattractant (22) or the direction of cell motion relative to that gradient (25, 36). In this model we assume both constant persistence time and constant cell speed so that the size of a step will be constant. Cell speeds can vary in vitro in response to chemical stimulation of the cell, a phenomenon known as chemokinesis (32). This complication will not be included in our analysis, as it would require a specific model for speed as a function of cell position relative to the target.

To include a bias in cell motion, different probabilities are assigned to motion in each direction. The probabilities are defined as shown in Fig. 2. Estimates of these probabilities can be obtained either by observation of many individual cell paths in vitro or by observation of the orientation behavior of cells near a target or in a known gradient of chemoattractant, as in the Zigmond bridge (37). The actual numbers used in the equation for encounter time will depend on the chemoattractant gradient around a target and the cell's ability to respond to it. A steep gradient of a strong attractant might result in a larger average value of p than would a shallow gradient of the same attractant, for example. Rather than focus on a particular type of gradient and attractant, in this paper we consider the effect on encounter times of varying these probabilities. Our results can then be related to various possible biological systems and compared to typically observed responses.

The probabilities p, q, and m are related to other measurable quantities that have been used to describe the directedness of cell motion: the chemotactic index and the chemotaxis coefficient. The chemotactic index, or CI, is defined as the net path length traversed by a cell toward a source divided by the total distance the cell has traveled (23). An index of one represents perfectly directed motion, and an index of zero represents completely random movement. The CI of neutrophils, for example, is about 0.85 under optimal experimental conditions (36). A cell taking N steps will move pN steps toward the target, qN steps away, and $2mN$ steps in the perpendicular direction. The net number of steps moved toward the source is, therefore, $(p - q)N$. For steps of constant length, the CI will be equal to the ratio of this net number of steps divided by the total number of steps, or $(p - q)$. Note that while the CI indicates the net amount of bias in cell motion, it does not uniquely describe the path of a cell since it is independent of the probability m. The chemotaxis coefficient used by Alt (2) and Lauffenburger (18) to describe the directed motion of a population of cells can be calculated from population migration data obtained using the linear under-agarose assay for chemotaxis, or from orientation data obtained using the Zigmond bridge (37). This coefficient was first defined by Keller and Segel (15) and is roughly proportional to the chemotactic index described above (24).

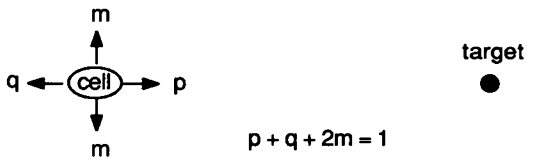

FIGURE 2. Probabilities of motion in different directions.

The position of the cell relative to the target is described in polar coordinates, as shown in Fig. 3, where r is the distance from the cell to the target, and θ describes the cell's position relative to some arbitrary reference vector. Motion toward or away from the target changes r by a step length δ, but does not change θ. A step in the perpendicular direction is mainly a change in θ, but the cell also travels a small distance away from the target, dr. If the distance traveled along the arc of constant radial distance from the target is equal to δ, then the incremental change in θ corresponding to this step, $d\theta$, is equal to the ratio of this arc length to the radial position of the arc, δ/r. Geometric arguments, detailed in Appendix A, then lead to the conclusion that dr is approximately equal to $\delta^2/2r$.

A difference equation for the encounter time of a nonrandomly moving cell reaching a target as a function of the initial distance between them can be derived using a modification and extension of the approach originally suggested by Berg and Purcell for nonbiased motion of a particle near an absorber (3). The mean capture time, or encounter time, for a cell at any position is equal to the time elapsed as the cell moves to a new position (the persistence time) plus the encounter time associated with that new position. Since the cell can move to any of four new positions, the encounter time associated with the cell's new location is the weighted average of the encounter times for each position to which it can move, and the weighting factor for each position is the probability that the cell will move there. The resulting difference equation for W, the

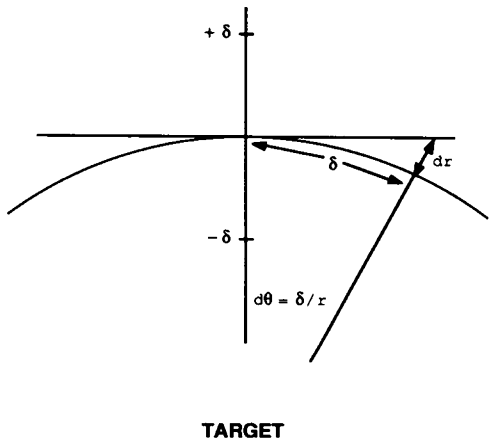

FIGURE 3. Description in polar coordinates of the positions available to the cell as it makes a step.

encounter time, is

$$W(r,\theta) = \tau + p\,W(r-\delta,\theta) + q\,W(r+\delta,\theta) + m\,W(r+\delta^2/2r,\theta+\delta/r) + m\,W(r+\delta^2/2r,\theta-\delta/r). \quad (2)$$

If we take the limit of this equation as step size becomes much smaller than the size of the unit space surrounding the target and for step times much smaller than the time of observation of the system, a differential equation for the mean capture time as a function of starting position is obtained. The resulting equation is

$$\frac{d^2W}{dr^2} + \left[\frac{2(q-p)}{\delta(p+q)} + \frac{(1-p-q)}{r(p+q)}\right]\frac{dW}{dr} = \frac{-2}{s^2\tau(p+q)}, \quad (3a)$$

with the boundary conditions

$$W(A) = 0 \quad (3b)$$

$$\frac{dW}{dr}(R) = 0, \quad (3c)$$

where s is cell speed, τ is directional persistence time (step time), δ is step size (equal to $s\tau$), R is outer radius of space around target, and A is contact radius.

The combination of speed squared and persistence time on the right-hand side of this equation is equivalent to a random motility coefficient for the cell (15, 18). This parameter describes the randomness of the cell's motion and is analogous to a diffusion coefficient for molecular motion. If we make the following substitution,

$$\mu = s^2\tau/4, \quad (4)$$

the effects of cell speed and persistence time on the encounter time are incorporated in the two parameters of step size, δ, and random motility coefficient, μ.

The boundary condition at $r = A$ follows from the fact that the encounter time is zero when the cell has reached the contact radius. The second boundary condition is one of symmetry. For the above equation to describe events in a unit space that is adjacent to other such spaces, we require that the normal derivative of the encounter time evaluated at the outer boundary of the unit space be zero to allow the calculated encounter time to be continuous from one unit space to the next.

The result that encounter time is independent of angular position of the cell relative to some arbitrary vector starting at the target is actually implicit in our physical picture of the target as a source of some chemical attractant that influences the direction of the cell. The concentration profile of this attractant will be radially symmetric around the target, with concentration decreasing as distance from the target increases. If we assume that the target and cell densities are low, then this concentration profile will be unaffected by the presence of other targets and cells. Since the chemoattractant gradient is uniform in the θ direction, there will be no change in the cell's encounter time with θ.

To put this equation in dimensionless form, scaling factors must be chosen for the radial position of the cell and the encounter time. Distance from the target will be scaled to the outer radius of the unit space, R. Encounter time must be made dimensionless with respect to another parameter that includes time. Possible choices for this include the persistence time, the cell speed, and the random motility coefficient. Scaling to persistence time is rejected immediately because this time is assumed to be much smaller than the encounter time in the limiting case for which this differential equation was derived. Dimensionless equations can be obtained for each of the two remaining choices of characteristic time: speed and random motility coefficient. The approximate solution of each equation using the ratio of the step size to the radius of the unit space as a small parameter may be performed using a singular perturbation approach. To zeroth order in step size, the expression for encounter time scaled to speed is valid only near the target, and the expression for encounter time scaled to the random motility coefficient is valid only at the outer boundary of the unit space. These approximate solutions are presented in Appendix B. Exact solution of the encounter time equation is presented here for encounter time scaled to speed, as this is a commonly measured parameter characteristic of individual cells, while the random motility coefficient is most accurately obtained from and applied to cell population responses.

The resulting equation written in scaled form is

$$\epsilon\frac{d^2\omega}{d\rho^2} + \left[2\frac{(q-p)}{(p+q)} + \epsilon\frac{(1-p-q)}{\rho(p+q)}\right]\frac{d\omega}{d\rho} = \frac{-2}{(p+q)}, \quad (5a)$$

with the boundary conditions

$$\omega(A/R) = 0 \quad (5b)$$

$$\frac{d\omega}{d\rho}(1) = 0, \quad (5c)$$

where ω is dimensionless mean capture time (equal to Ws/R), ρ is r/R, and ϵ is δ/R. Now the effects of cell speed and persistence time on the dimensionless encounter time are incorporated in the single parameter ϵ.

Solution of this inhomogeneous second-order linear equation is performed using a variation of parameters method (4). The result is a closed form solution made up of three integrals that must be evaluated numerically for most choices of the parameters involved. This equation is

$$\omega = \frac{2}{\epsilon(p+q)}\left[\int_{A/R}^{\rho} e^{-k\xi}\,\xi^b \int_{A/R}^{\xi} e^{ks}\,s^{-b}\,ds\,d\xi + \left(\int_{A/R}^{\rho} e^{ks}\,s^{-b}\,ds\right)\left(\int_{\rho}^{1} e^{-k\xi}\,\xi^b\,d\xi\right)\right], \quad (6a)$$

where

$$k = \frac{2(p-q)}{\epsilon(p+q)} \tag{6b}$$

$$b = \frac{1}{(p+q)} - 1. \tag{6c}$$

We compute these integrals by either Gauss-Legendre or Gauss-Laguerre quadrature (5), depending on the limits of integration and the form of the integrand.

There are certain sets of probabilities p, q, and m that permit an exact solution of this differential equation to be determined, as outlined below.

Case A: Motion in One Dimension ($m = 0$)

When m is equal to zero, the problem reduces to a description of motion in one dimension, and the encounter time is calculated as follows:

$$\omega = \frac{\rho - A/R}{(p-q)} - \frac{\epsilon e^{-k}}{2(p-q)^2}(e^{k\rho} - e^{kA/R}). \tag{7}$$

When $p = 1$, the cell moves directly to the target, and we would expect that the encounter time will equal the distance traveled by the cell divided by its speed. For this choice of probabilities, the above equation becomes

$$\omega = \rho - A/R - \frac{\epsilon e^{-2/\epsilon}}{2}(e^{2\rho/\epsilon} - e^{2A/\epsilon R}). \tag{8}$$

For small step size, this reduces to the anticipated result:

$$\omega = \rho - A/R, \text{ or } W = (r - A)/s. \tag{9}$$

Case B: $p = q$

When all three probabilities p, q, and m are equal, the resulting encounter time corresponds to purely random motion of the cell. As expected, this result is the same as that obtained by Berg and Purcell for their description of random particle motion (3).

$$\omega = \frac{2}{\epsilon}\left\{\ln(\rho R/A) + \frac{1}{2}[(A/R)^2 - \rho^2]\right\}. \tag{10}$$

If p and q are equal to each other but are not equal to 0.25, the following equation is obtained for encounter time as a function of initial position of the cell:

$$\omega = \frac{2}{\epsilon}\left\{\frac{1}{C}(\rho^C - (A/R)^C) + \frac{1}{2}[(A/R)^2 - \rho^2]\right\}, \tag{11a}$$

where

$$C = 2 - \frac{1}{(2p)}. \tag{11b}$$

The dependence of the encounter time on the actual position of the cell can be removed by averaging the encounter time over all possible distances between the cell and target:

$$\bar{\omega} = \frac{2\int_{A/R}^{1}\omega(\rho)\,\rho\,d\rho}{1 - (A/R)^2}. \tag{12}$$

Instead of integrating Eq. 6a to obtain this surface averaged encounter time, we return to the original differential Eq. 5a, multiply each term by a factor of ρ, and integrate each term over position, ρ. A similar equation is obtained by multiplying Eq. 5a by ρ^2 and integrating over position. The resulting two equations are combined to provide an expression for surface averaged encounter time that requires evaluating only two integrals.

$$\bar{\omega} = \frac{1}{k[1 - (A/R)^2]} \cdot \left\{\frac{-g}{3}[1 - (A/R)^3] - \frac{(b-2)g}{2k}[1 - (A/R)^2] + (A/R)\frac{d\omega}{d\rho}(A/R)\left[(A/R) + \frac{(b-2)}{k}\right] + \omega(1)\left[k - \frac{(b-1)(b-2)}{k}\right]\right\}, \tag{13a}$$

where

$$g = \frac{2}{\epsilon(p+q)} \tag{13b}$$

$$\frac{d\omega}{d\rho}(A/R) = \frac{ge^{k(A/R)}\int_{A/R}^{1} e^{-k\xi}\xi^b\,d\xi}{(A/R)^b} \tag{13c}$$

$$\omega(1) = g\int_{A/R}^{1} e^{-k\xi}\xi^b \int_{A/R}^{\xi} e^{ks}s^{-b}\,ds\,d\xi. \tag{13d}$$

RESULTS AND DISCUSSION

In the previous section, we obtained an expression for cell–target encounter time as a function of cell speed and persistence time, directional orientation bias of the cell, and the dimensions of the area in which the cell searches for its target. We now evaluate the influence that these properties have on the encounter time.

Our results show that an increase in cell speed or persistence time decreases the encounter time. Fig. 4 presents dimensionless average encounter time for completely random and perfectly directed motion as a function of the dimensionless step size, ϵ, which is proportional to the product of speed and persistence time. The separate effects of cell speed and persistence time on the random encounter time are shown more clearly in Fig. 5, a plot of average encounter time (in hours) as a function of cell speed. The curves are parameterized in persistence times believed to be characteristic for cells such as polymorphonuclear leukocytes (13, 38) and alveolar macrophages. The

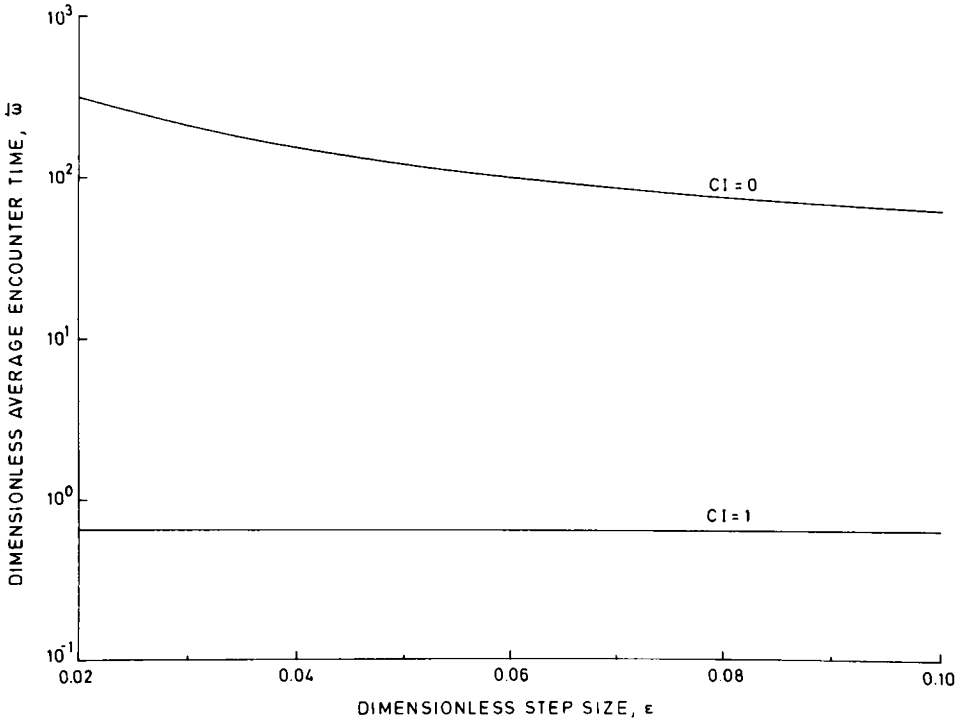

FIGURE 4. Effect of dimensionless step size on dimensionless average encounter time. Curves are parameterized in chemotactic index, CI. $A/R = 0.02$.

range of cell speeds shown corresponds to speeds reported for polymorphonuclear leukocytes (22, 32), monocytes (16, 17), macrophages (33), and lymphocytes (32). In both graphs we see that random encounter time is more sensitive to changes in these parameters than is the encounter time for directed motion. It is also clear that increasing speed and persistence time in the realistic range of values used here does not make random encounter times comparable to directed times. The amount of directional bias in cell motion has a greater influence on encounter time than do these motility parameters.

In general, an increase in the amount of directional orientation bias will decrease encounter time. The amount of bias is indicated by p, the probability of the cell moving to the target, and by the chemotactic index, which is defined as the difference between p and q, the probability of the cell moving directly away from the target. While the chemotactic index, CI, does not uniquely describe a cell

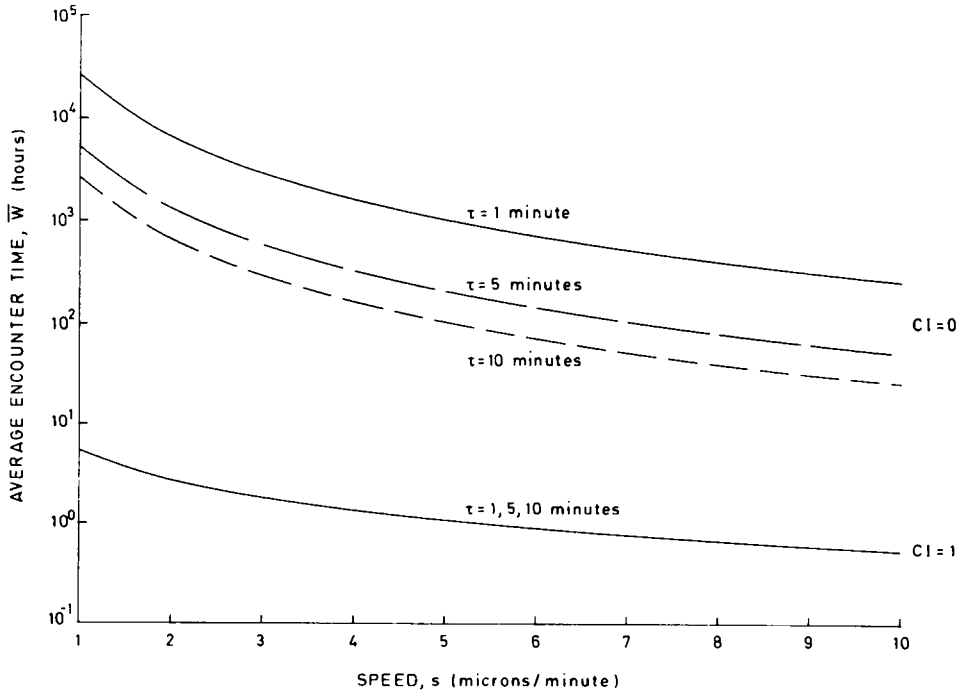

FIGURE 5. Effect of cell speed on average encounter time. Curves are parameterized in persistence time, τ, and CI. $R = 500.0\ \mu m$, $A/R = 0.02$, $\epsilon \leq 0.2$.

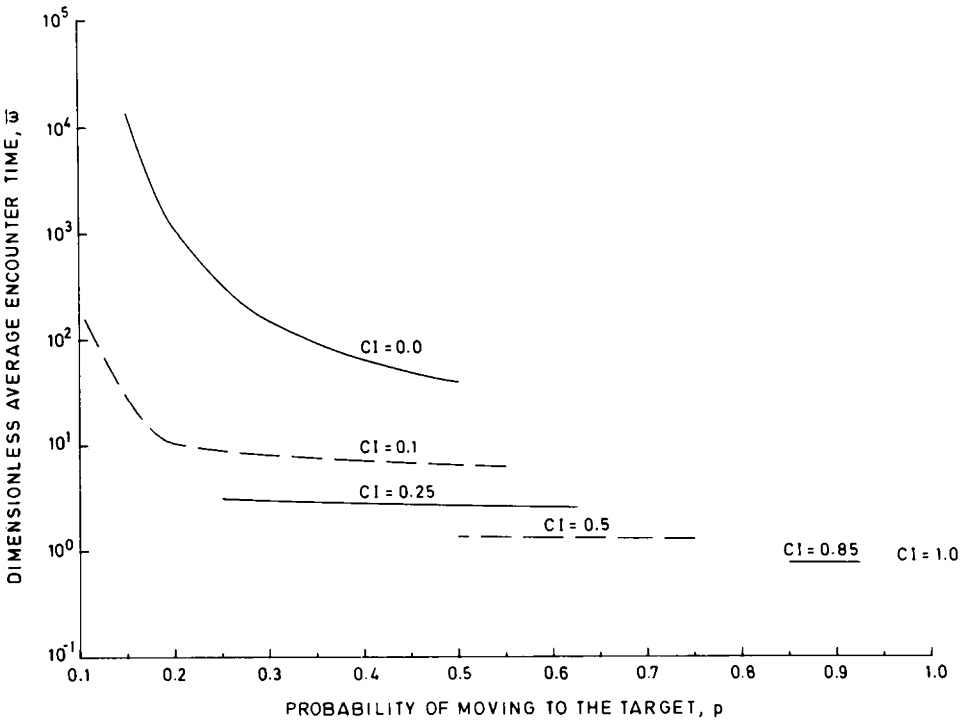

FIGURE 6. Effect of the probability of the cell moving directly toward the target on dimensionless average encounter time. Curves are parameterized in CI. CI = $p - q$, A/R = 0.02, ϵ = 0.02.

path, it is equivalent to the net amount of orientational bias exhibited by the cell over its entire path. Fig. 6 presents the variation of the dimensionless average encounter time with the probability p for a range of CI. We see that encounter time decreases as the amount of bias increases, and that an increase in the net chemotactic bias, CI, leads to a decrease in sensitivity of encounter time to the actual value of the probability p.

It is possible to select one point on each of these curves of constant CI by choosing the remaining probability, m. This reduces the problem of describing cell motion bias from having two degrees of freedom to having one. One possible choice is to set m equal to q so that the cell is equally likely to move no closer to the target as it is to move directly away. With this choice, it is possible to obtain both the solution corresponding to $p = 1$ (perfectly directed motion)

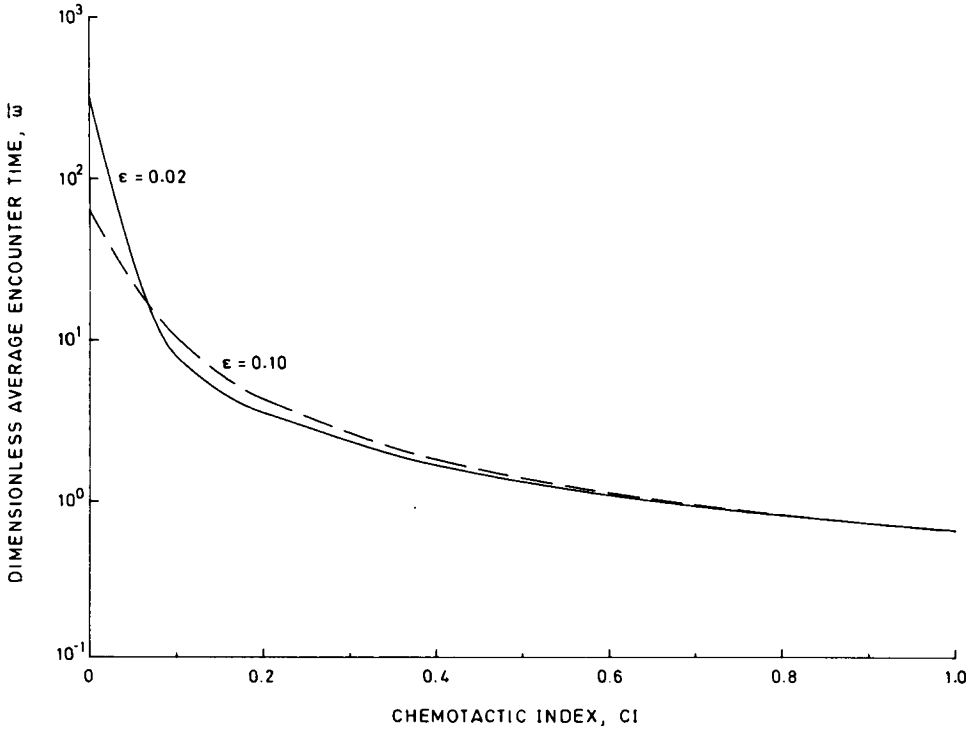

FIGURE 7. Effect of chemotactic index on dimensionless average encounter time. Curves are parameterized in two choices of dimensionless step size, ϵ. $q = m$, A/R = 0.02.

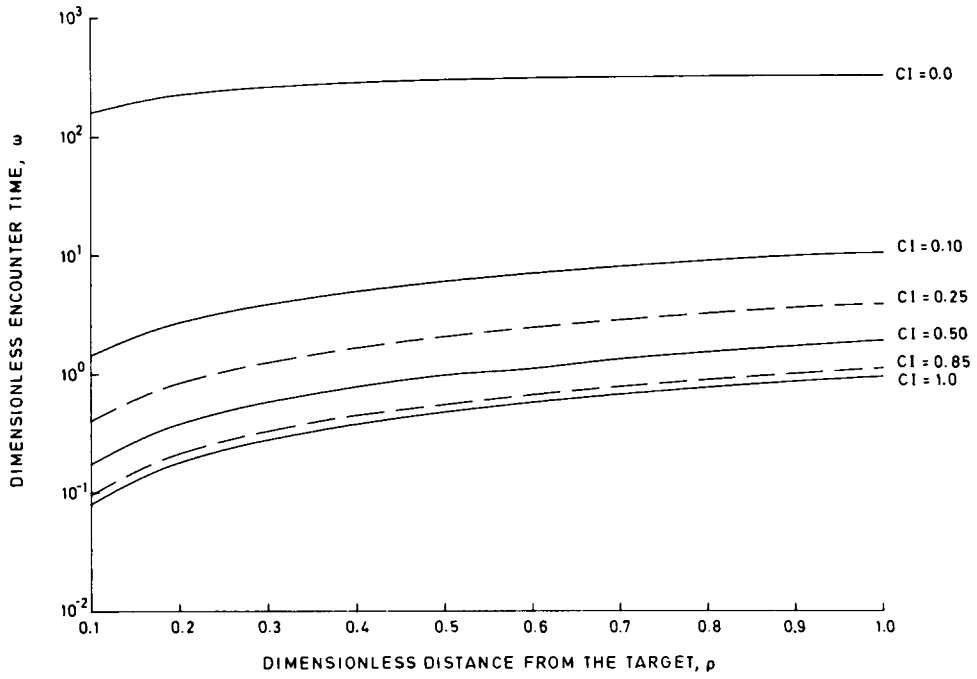

FIGURE 8. Effect of dimensionless distance from the target on dimensionless encounter time. Curves are parameterized in CI. $q = m$, $A/R = 0.02$, $\epsilon = 0.02$.

shown as a point in Fig. 6, as well as the encounter time for random motion that corresponds to Berg and Purcell's result (3). If m is chosen to be equal to some particular constant value, or if m is chosen as some constant proportion of either p or q, only one of these limiting cases could be obtained. If m is chosen to be always zero, the description of cell motion is reduced to one dimension. Setting q equal to m appears to be the most reasonable choice of probabilities to reduce the number of degrees of freedom in this description of cell directional bias.

We use this choice of probabilities in Fig. 7 to present the effect of the net amount of bias, CI, on dimensionless average encounter time. As the chemotactic index increases from the limit of random motion, there is a great reduction in dimensionless encounter time—a decrease of one to two orders of magnitude for an increase in CI merely from 0 to 0.2. As the CI increases further, there is a much smaller proportional change in encounter time. Clearly, this result shows that it is not necessary for a cell to move perfectly toward the target to achieve encounter times

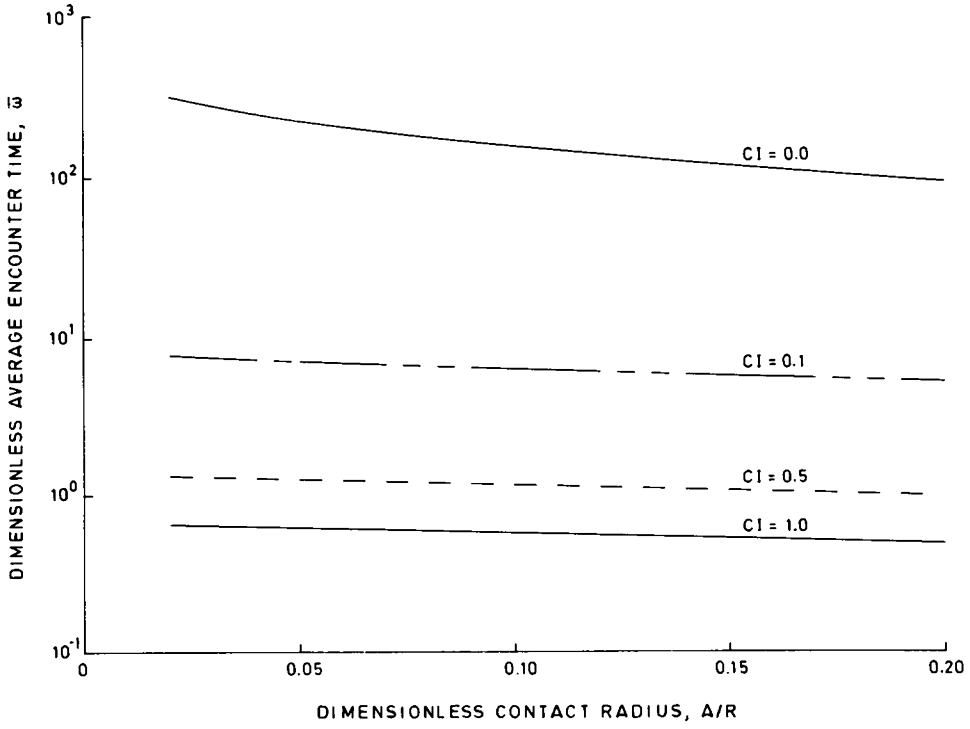

FIGURE 9. Effect of dimensionless contact radius on dimensionless average encounter time. Curves are parameterized in CI. $q = m$, $\epsilon = 0.02$.

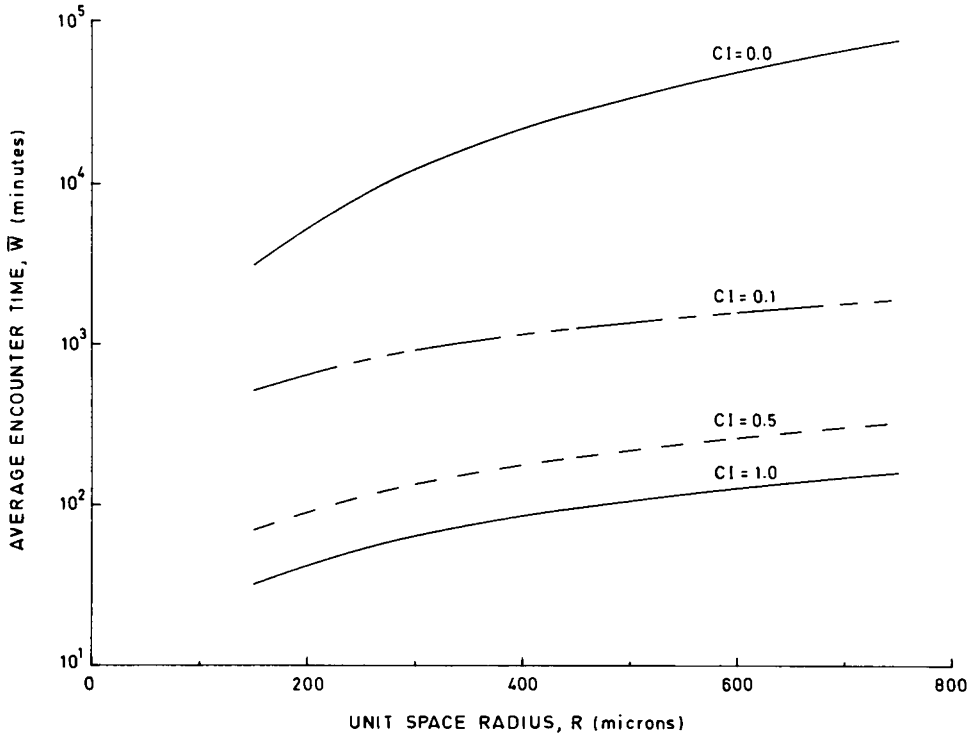

FIGURE 10. Effect of unit space radius on average encounter time. Curves are parameterized in CI. $q = m$, $s = 3$ μm/min, $\tau = 5$ min, $A/R = 0.02$, $\epsilon \leq 0.1$.

significantly shorter than those predicted for random motion. Chemotactic ability can be a great advantage to cells as they encounter targets, and a small amount of bias is nearly as good as perfectly directed motion in decreasing the encounter time. This may have important implications for the correlation of cell chemotactic defects with their consequences for the effective functioning of the host immune defense system.

In Fig. 7 we can again compare the effects of directional bias and step size on encounter time. As in Fig. 4, we see that random encounter time does vary with step size, and to a greater extent than do encounter times for values of CI greater than 0.1. However, an increase in step size by a factor of five still results in a significantly larger encounter time for random motion than for motion with even a moderate amount of bias. The crossing of the curves for different step sizes is due to slight instabilities in the numerical integral evaluation procedure.

The final category of parameters that influence encounter times are those that describe the unit space: the starting position of the cell relative to the target, the contact radius, and the outer radius of the unit space. In Fig. 8 we see that dimensionless encounter time increases with starting distance from the target, as we would expect. This graph also reemphasizes the observation that encounter time is more sensitive to changes in bias near the limit of completely random motion than when motion is more directed. The effect of changing contact radius on dimensionless average encounter time is shown in Fig. 9. Encounter time is decreased somewhat as contact radius increases, but only by about 20% over the range of contact radius shown here if the cell is moving with even a small amount of chemotactic orientation bias. Therefore, variations in cell size or shape due to membrane activity should have a relatively minor effect on our encounter time estimates. Finally, Fig. 10 presents the variation of average encounter time with the outer radius of the unit space with curves parameterized in CI. When the size of the unit space is related to target density as shown in Eq. 1, a large radius corresponds to a low surface density of targets. As target density decreases (R increases), encounter time increases, with a more dramatic change seen in random motion encounter time than in times calculated for even a small amount of chemotactic bias. Neither starting position nor contact radius is as effective in changing encounter time as is the amount of directional orientation bias. A decrease in the radius of the unit space, however, can reduce the order of magnitude of the random encounter time to a value comparable to that for directed motion.

CONCLUSIONS

Cells of the immune system must encounter other cells or foreign material to perform many of their functions. Thus, the efficiency with which a cell can come into contact with its target may greatly influence the overall ability of the host to defend against disease. Some of these cells have demonstrated an ability to move chemotactically and it is possible that this ability enhances the rate at which targets are encountered in vivo. We have described a model for cell motion in two dimensions in the vicinity of a target that predicts the time required for encounter to occur if the cell moves either completely randomly or with some amount of chemotactic directional bias, up to the limit of perfectly directed motion.

The model we have presented predicts the effects that changes in cell speed, persistence time, chemotactic directional bias, and the dimensions of the area available to the cell have on the encounter time. The most important of our results is the prediction that a small amount of directional bias in cell motion reduces the encounter time considerably from that calculated for a randomly moving cell. This indicates that even a small amount of chemotactic ability is a substantial advantage to scavenging cells, even when their response is far from perfect. The order of magnitude of the random encounter times we calculate implies that some chemotactic bias is needed to permit cells to encounter their targets efficiently in the body, but a perfect chemotactic response would not be required.

Our results are helpful in examining encounter in the context of the other steps involved in overall cell functions such as target killing or phagocytosis. The encounter time can be compared with characteristic times for each of the other steps, and the largest characteristic time will correspond to the rate-limiting step. For example, observation of macrophage phagocytosis of particles and bacteria indicates that the characteristic time required for these cells to ingest foreign material is of the order of 5–10 min (14, 19–21). Characteristic times calculated here for encounter in two dimensions depend on the choice of chemotactic index and target density. Fig. 11 shows how average encounter time varies with particle density for two choices of macrophage speeds in the limits of directed and random motion. Since these times are larger than the estimated characteristic time for phagocytosis, encounter may be the rate-limiting step in the process of target clearance.

We can further understand the importance of chemotaxis for host defense by considering its influence on encounter rates and on the rates of overall processes that involve encounter. The surface-averaged encounter time we calculate is approximately equivalent to an inverse rate constant for the encounter process occurring among larger numbers of cells and targets (29). When the size of the unit space is based on the instantaneous surface density of targets so that the rate constant depends implicitly on target density, the encounter rate will be equal to the product of the immune cell surface density at any time and this encounter rate constant. This encounter rate can be used in describing the overall process of phagocytosis, for example, as a sequence of steps including encounter of the target, binding of encountered targets, and ingestion. The resulting dynamic model will predict target density as a function of time and cell motility properties. Since our encounter time is derived for the case of single cell and single target encounter, its application to larger systems will provide an approximation to the actual encounter rate constant. The validity of this approximation can be evaluated by comparison of our results to experiment or to computer simulation of multiple cell and target behavior.

A valuable application of our results is in the correlation of defective chemotaxis of immune cells with incidence of infection. Whether such a defect will cause impairment of the immune response depends not only on the magnitude of the defect, but also on the situation in which encounter occurs in the host and the rates of cellular processes that follow encounter. As an example, consider the clearance of bacteria from the lung. Here, typical initial experimental bacterial challenges (11) are equivalent to fairly large unit spaces (the upper range of R in Fig. 10), and encounter is

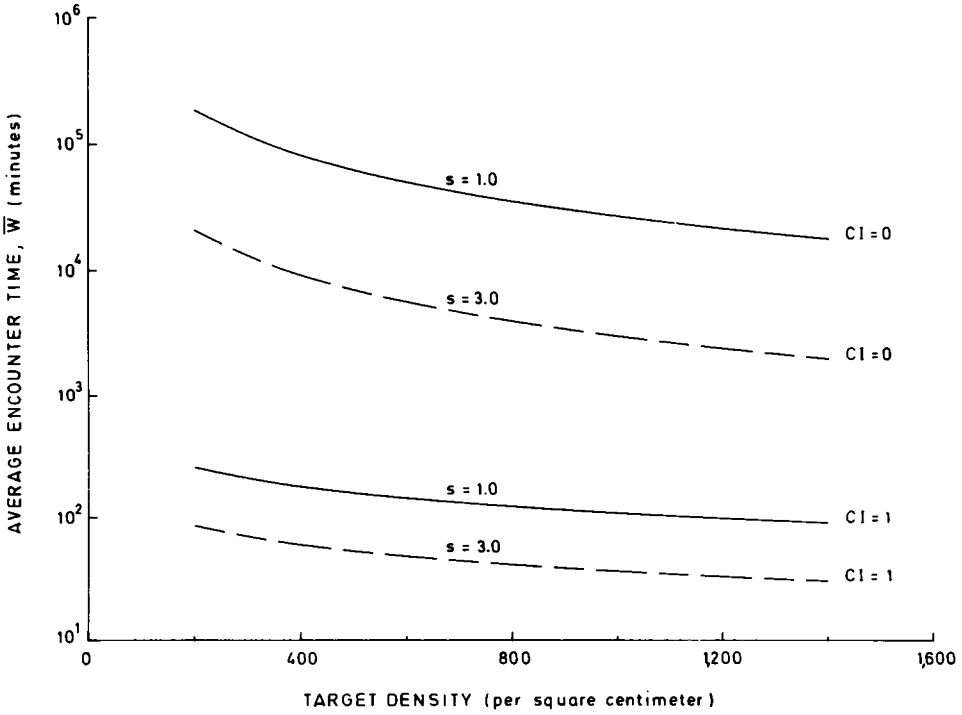

FIGURE 11. Effect of target density on average encounter time. Curves are parameterized in two cell speeds, 1 and 3 μm/min, and in CI. A = 10.0 μm, τ = 5 min.

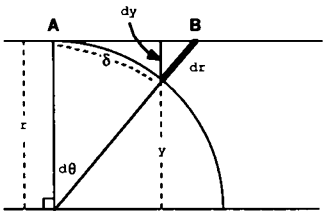

FIGURE 12. One quadrant of a unit space of radius r. See Appendix A for discussion.

probably the rate-limiting step relative to ingestion. Our analysis predicts that an observed decrease in alveolar macrophage chemotactic index to 50% of its normal value would cause an increase in encounter time from 5 to 10 h if the CI is normally 0.7. To determine the resulting effect on lung clearance of the observed chemotactic defect, both the normal and increased encounter times we calculate must be used in a dynamic clearance model of the type described above.

APPENDIX A

Calculation of Incremental Change in Radial Position

In Fig. 12 we present a view of one quadrant of a circle of radius r surrounding a target. We let a cell at point A take a step to the right, to point B, which corresponds to moving a distance δ along the arc of the circle shown and moving through an angle $d\theta$ relative to its original position. Arc length δ is related to $d\theta$ as shown below:

$$d\theta = \frac{\delta}{r}. \tag{A1}$$

We calculate the vertical distance y as a function of θ as follows:

$$y = r \sin (90 - d\theta) = r \cos d\theta, \tag{A2}$$

and expand the cosine of the small angle $d\theta$ in a Taylor series:

$$y = r\left[1 - \frac{(d\theta)^2}{2} + \cdots\right]. \tag{A3}$$

Since $y + dy = r$, or $y = r - dy$, then

$$dy = r\frac{(d\theta)^2}{2} \tag{A4}$$

and for a step size δ that is small relative to r, dr will be approximately equal to dy:

$$dr \approx r\frac{(d\theta)^2}{2} = \frac{\delta^2}{2r}. \tag{A5}$$

APPENDIX B

Solutions Using Alternative Scaling for Encounter Time

When encounter time is scaled to speed as follows:

$$\omega = Ws/R, \tag{B1}$$

and the distance to the target is scaled to R, this differential equation for dimensionless encounter time is obtained:

$$\frac{d^2\omega}{d\rho^2} + \left[2\frac{(q-p)}{(p+q)}\frac{R}{\delta} + \frac{(1-p-q)}{\rho(p+q)}\right]\frac{d\omega}{d\rho} = \frac{-2}{(p+q)}\frac{R}{\delta}. \tag{B2}$$

Let δ/R be the small parameter in a perturbation expansion, so that

$$\omega = \omega_0 + \frac{\delta}{R}\omega_1 + \cdots \tag{B3}$$

To zeroth order in this parameter, dimensionless encounter time is calculated from:

$$2\frac{(q-p)}{(p+q)}\frac{d\omega_0}{d\rho} = \frac{-2}{(p+q)}. \tag{B4}$$

This equation can satisfy only the boundary condition of zero encounter time at the target, so that:

$$\omega_0 = \frac{\rho - A/R}{p-q}. \tag{B5}$$

When encounter time is scaled instead to the random motility coefficient, μ, as follows:

$$\omega = W\mu/R^2, \tag{B6}$$

the resulting differential equation for dimensionless encounter time is:

$$\frac{d^2\omega}{d\rho^2} + \left[2\frac{(q-p)}{(p+q)}\frac{R}{\delta} + \frac{(1-p-q)}{\rho(p+q)}\right]\frac{d\omega}{d\rho} = \frac{-1}{2(p+q)}. \tag{B7}$$

Using the same expansion for dimensionless encounter time in δ/R, the zeroth order solution is calculated from:

$$2\frac{(q-p)}{(p+q)}\frac{d\omega_0}{d\rho} = 0. \tag{B8}$$

This can satisfy only the boundary condition of no change in encounter time across the outer boundary of the unit space, so that:

$$\omega_0 = \text{constant}. \tag{B9}$$

We thank Ronald Daniele, Wolfgang Alt, and Leah Edelstein Keshet for many helpful discussions.

The authors gratefully acknowledge the financial support of National Science Foundation Grant DCB83-03017, and National Institutes of Health RCDA Award DE-00143 to D.A.Lauffenburger.

Received for publication 11 August 1986 and in final form 29 December 1986.

REFERENCES

1. Allan, R. B., and P. C. Wilkinson. 1978. A visual analysis of chemotactic and chemokinetic locomotion of human neutrophil leukocytes. *Exp. Cell Res.* 111:191–203.
2. Alt, W. 1980. Biased random walk models for chemotaxis and related diffusion approximations. *J. Math. Biol.* 9:147–177.
3. Berg, H. C. and E. M. Purcell. 1977. Physics of chemoreception. *Biophys. J.* 20:193–219.
4. Boyce, W. E., and R. C. DiPrima. 1977. Elementary Differential Equations and Boundary Value Problems. 3rd ed. John Wiley & Sons, Inc., New York.
5. Carnahan, B., H. A. Luther, and J. O. Wilkes. 1969. Applied Numerical Methods. John Wiley & Sons, Inc., New York.

6. Clark, W. R. 1983. The Experimental Foundations of Modern Immunology. 2nd ed. John Wiley & Sons, Inc., New York.
7. Dauber, J. H., and R. P. Daniele. 1978. Chemotactic activity of guinea pig alveolar macrophages. *Am. Rev. Respir. Dis.*117:673–684.
8. Dunn, G. A. 1982. Characterizing a kinesis response: time averaged measures of cell speed and directional persistence. *In* Leukocyte Locomotion and Chemotaxis, Agents, and Actions Supplements, 12. H. Keller and G. Till, editors. Birkhauser Verlag, Boston.
9. Falk, W., and E. J. Leonard. 1980. Human monocyte chemotaxis: migrating cells are a subpopulation with multiple chemotaxin specificities on each cell. *Infect. Immun.* 29:953–959.
10. Goel, N. S., and N. Richter-Dyn. 1974. Stochastic Models in Biology. Academic Press, Inc., New York.
11. Goldstein, E., W. Lippert, and D. Warshauer. 1974. Pulmonary alveolar macrophage: defender against bacterial infection of the lung. *J Clin. Invest.* 54:519–528.
12. Green, G. M., and E. H. Kass. 1964. The role of the alveolar macrophage in the clearance of bacteria from the lung. *J. Exp. Med.* 119:167–179.
13. Gruler, H., and B. D. Bultmann. 1984. Analysis of cell movement. *Blood Cells (Berl.).* 10:61–77.
14. Jonsson, S., D. M. Musher, A. Chapman, A. Goree, and E. C. Lawrence. 1985. Phagocytosis and killing of common bacterial pathogens of the lung by human alveolar macrophages. *J. Infect. Dis.* 152:4–13.
15. Keller, E. F., and L. A. Segel. 1971. Models for chemotaxis. *J. Theor. Biol.* 30:225–234.
16. Kirby, J. A., A. J. Suckling, and M. G. Rumsby. 1983. Chronic relapsing experimental allergic encephalomyelitis: the presence in the cerebrospinal fluid of factors chemotactic for monocytes. *J. Neuroimmunol.* 5:271–281.
17. Lackie, J. M., C. M. Urquhart, A. F. Brown, and J. V. Forrester. 1985. Studies on the locomotory behavior and adhesive properties of mononuclear phagocytes from blood. *Brit. J. Haematol.* 60:567–581.
18. Lauffenburger, D. 1983. Measurement of phenomenological parameters for leukocyte motility and chemotaxis. *In* Agents and Actions Supplements. Vol. 12. H. U. Keller and G. O. Till, editors. Birkhauser Verlag, Basel.
19. Lehnert, B. E., and P. E. Morrow. 1985. The initial lag in phagocytic rate by macrophages in monolayer is related to particle encounters and binding. *Immunol. Invest.* 14:515–521.
20. Lehnert, B. E., and C. Tech. 1985. Quantitative evaluation of opsonin-independent phagocytosis by alveolar macrophages in monolayer using polystyrene microspheres. *J. Immunol. Methods.* 78:337–344.
21. Leijh, P. C. J., M. Th. van den Barselaar, and R. van Furth. 1981. Kinetics of phagocytosis and intracellular killing of *Staphylococcus aureus* and *Escherichia coli* by human monocytes. *Scand. J. Immunol.* 13:159–174.
22. Maher, J., J. V. Martell, B. A. Brantley, E. B. Cox, J. E. Niedel, and W. F. Rosse. 1984. The response of human neutrophils to a chemotactic tripeptide (N-formyl-methionyl-leucyl-phenylalanine) studied by microcinematography. *Blood.* 64:221–228.
23. McCutcheon, M. 1946. Chemotaxis in leukocytes. *Physiol. Rev.* 26:319–336.
24. Nossal, R. 1980. Mathematical theories of topotaxis. *Lect. Notes Biomath.* 38:410–439.
25. Nossal, R., and S. H. Zigmond. 1976. Chemotropism indices for polymorphonuclear leukocytes. *Biophys. J.* 16:1171–1182.
26. Rosenstreich, D. L. 1981. The macrophage. *In* Cellular Functions in Immunity and Inflammation. J. J. Oppenheim, D. L. Rosenstreich, and M. Potter, editors. Elsevier North-Holland, New York.
27. Schwartz, L. W., and C. A. Christman. 1979. Alveolar macrophage migration: influence of lung lining material and acute lung insult. *Am. Rev. Respir. Dis.* 120:429–439.
28. Sorokin, S. P. 1977. Phagocytes in the lungs: incidence, general behavior, and phylogeny. *In* Respiratory Defense Mechanisms. Part 2. J. D. Brain, D. F. Proctor, and L. M. Reid, editors. Marcel Dekker, New York.
29. Szabo, A., K. Schulten, and Z. Schulten. 1980. First passage time approach to diffusion controlled reactions. *J. Chem. Phys.* 72:4350–4357.
30. Toews, G. B., G. N. Gross, and A. K. Pierce. 1979. The relationship of inoculum size to lung bacterial clearance and phagocytic cell response in mice. *Am. Rev. Respir. Dis.* 120:559–566.
31. Warheit, D. B., L. H. Hill, and A. R. Brody. 1984. Surface morphology and correlated phagocytic capacity of pulmonary macrophages lavaged from the lungs of rats. *Exp. Lung Res.* 6:71–82.
32. Wilkinson, P. C. 1982. Chemotaxis and Inflammation. 2nd ed. Churchill Livingstone, New York.
33. Wilkinson, P. C. 1982. Visual observations of chemotaxis and chemotropism in mouse macrophages. *Immunobiol.* 161:376–384.
34. Wilkinson, P. C., D. M. V. Parrott, R. J. Russell, and F. Sless. 1977. Antigen-induced locomotor responses in lymphocytes. *J. Exp. Med.* 145:1158–1168.
35. Zeligs, B. J., L. S. Nerurkar, and J. A. Bellanti. 1984. Chemotactic and candidacidal responses of rabbit alveolar macrophages during postnatal development and the modulating roles of surfactant in these responses. *Infect. Immun.* 44:379–385.
36. Zigmond, S. H. 1974. Mechanisms of sensing chemical gradients by polymorphonuclear leukocytes. *Nature (Lond.).* 249:450–452.
37. Zigmond, S. H. 1977. Ability of polymorphonuclear leukocytes to orient in gradients of chemotactic factors. *J. Cell Biol.* 75:606–616.
38. Zigmond, S. H., R. D. Klausner, R. Tranquillo, and D. A. Lauffenburger. 1985. Analysis of the requirements for time-averaging of the receptor occupancy for gradient detection by polymorphonuclear leukocytes. *In* Membrane Receptors and Cellular Regulation. 347–356.